

Stress and strain distribution on denture-bearing area of distal extension removable partial denture and stress of the abutment tooth: A finite element analysis

Dalanporn Kaewkumnerd¹, Ekachai Chaichanasiri², Tharee Champirat³,
Pirasut Rodanant³

¹ Residency Training Program in General Dentistry, Faculty of Dentistry, Mahidol University, Bangkok, Thailand

² Department of Mechanical Engineering, Faculty of Engineering, Mahidol University, Nakhon Pathom, Thailand

³ Department of Advanced General Dentistry, Faculty of Dentistry, Mahidol University, Bangkok, Thailand

Objectives: This study investigated the distribution pattern and magnitude of stress and strain in the denture-bearing area and the abutment tooth upon the axial loading on the artificial tooth of a distal extension removable partial denture (RPD).

Materials and Methods: A 3D model of a Kennedy Class II mandibular arch was digitally created. Using finite element analysis software, the pattern and magnitude of stress and strain distribution were observed upon the application of an axial occlusal load of 100 N on the artificial teeth on the denture base (teeth 35, 36, and 37). The stress and strain distribution were analyzed separately when a force was applied on each artificial tooth. The descriptive explanation comparing the pattern and magnitude of stress and strain distribution was reported.

Results: The highest magnitude of stress and strain was observed when the axial load was applied on artificial tooth 35. A significant stress and strain distribution was observed in the cortical bone around the posterior region beneath the denture base. At the abutment tooth, the greatest stress distribution was found around the cervical area of the distobuccal tooth aspect. Interestingly, there was a decrease in the magnitude of stress and strain in the cortical bone and abutment tooth as the load was shifted posteriorly.

Conclusions: This study demonstrated that the location of the axial load on the denture base of the distal extension RPD did affect the magnitude of stress and strain and its distribution pattern. Appropriate design and consideration on the usage of distal extension RPD seemingly reduce the detrimental effect on the supporting periodontium and the abutment tooth.

Keywords: distal extension removable partial denture, finite element analysis, strain, stress

How to cite: Kaewkumnerd D, Chaichanasiri E, Champirat T, Rodanant P. Stress and strain distribution on denture-bearing area of distal extension removable partial denture and stress of the abutment tooth: A finite element analysis. M Dent J 2025;45(2): 139-148.

Introduction

The removable partial denture (RPD) has been introduced as an effective tooth substitution method in individuals who have lost their natural dentition. This restorative device has been claimed to be the most popular choice of dental substitution for Thai citizens in order to regain masticatory

function following the loss of their natural posterior teeth [1]. Nevertheless, during the course of RPD usage, some adverse effects affecting the RPD, tooth, and/or adjacent periodontium have been reported. A study utilizing cone-beam computed tomography revealed that the vertical and horizontal alveolar ridge resorption in both dentate and edentulous sites has occurred more

Corresponding author: Pirasut Rodanant

Department of Advanced General Dentistry, Faculty of Dentistry, Mahidol University,
6 Yothi Road, Ratchathewi, Bangkok 10400, Thailand

Tel: + 66 2200-7853 Email: pirasut.rod@mahidol.ac.th

Received: 13 March 2025

Revised: 28 May 2025

Accepted: 23 June 2025

in RPD wearers (whose tooth loss was classified as Kennedy Class II) than in non-RPD wearers [2]. The resorption of the alveolar ridge underneath the denture base of the RPD exerted a negative impact on two main essential requirements of the RPD, i.e., retention and stability, resulting in the loosening of the RPD. Loosening of the denture leads to common patient complaints, e.g., pain, feelings of discomfort, and reduced chewing ability. Eventually, these necessitate the repair of existing dentures or the re-fabrication of new dentures in order to regain patients' quality of life (QoL) [3]. Retention and stability are the two main requirements for an RPD to work effectively. The extension of the denture base onto the masticatory mucosa of the alveolar ridge is responsible for the stability of the RPD. This means that the design of a distal extension RPD should facilitate appropriate force distribution onto the supporting oral structures; i.e., tooth, periodontium, and oral mucosal tissues. In order to minimize the occurrence and/or progression of alveolar resorption and to maintain the RPD function and the health of the RPD and the supporting periodontium, it is important to understand the mechanics and to realize the capability of the RPD.

The purpose for conducting this study was to examine the distribution of stress and strain on the supporting structure underlying a denture base of a distal extension RPD and the force distribution on an abutment tooth of a distal extension RPD, considering the position of applied force on the artificial tooth of the denture base of a distal extension RPD utilizing finite element analysis (FEA). The results might raise dental practitioners' awareness concerning the fabrication of an effective and durable distal-extension RPD that will not exert negative force on oral structures supporting the distal extension RPD.

Materials and Methods

Model design and construction

The mandible of a human cadaver from the Department of Anatomy, Faculty of Dentistry, Mahidol University, was scanned using a CT scan machine (3D Accuitomo170, Morita, Japan). The assigned 3D model of Kennedy Classification II mandibular arch was generated and customized using Blender software (Blender, Netherlands).

CAD geometry

A cut-section of the 3D CAD model of the mandible was prepared for finite element analysis. A cortical layer of 2 mm thickness was modelled within the section boundary (Figure 1a). Covering the cortical layer was a gingival layer of 2 mm thickness (Figure 1b). Inside the cortical layer was a layer of cancellous bone. The natural teeth (teeth 34-47) were put in the model, leaving space distal to tooth 34 as an edentulous space to simulate Kennedy Classification II partially edentulous arch (Figure 1c).

The 3D CAD model of the lower removable partial denture was designed and simulated using 3-Shape dental manager client software (3-Shape A/S, Denmark) (Figure 1d). Tooth 34 was designed as an abutment tooth. Artificial teeth 35, 36, and 37 were put on Cobalt-chromium alloy (Co-Cr) RPD framework. An RPI clasp and rest were designed to engage on the abutment tooth. An acrylic denture base was designed to cover the denture-bearing area (Figure 1e).



Figure 1a



Figure 1b



Figure 1c



Figure 1d



Figure 1e

Figure 1 Fabrication and assembly of 3D model of mandible and lower RPD: 1a Cortical bone layer of 3D model of mandible; 1b Gingival layer of 3D model of mandible; 1c Assembly of cortical bone, natural teeth and gingival layer of 3D model of mandible; 1d Lower removable partial denture; 1e Assembly of 3D model of cortical bone, natural teeth, gingival layer and lower RPD.

FE modelling

The model of the prosthesis (skeleton and denture base), soft tissue (gingiva), and bone (cortical and cancellous) were meshed using Meshmixer software (Autodesk, USA) and Patran software (MSC. Software Corporation, USA) to generate a final mesh model before finite element analysis. The cut section of the finite element model is shown in Figure 2. A tetrahedral element was created from all layers of the model, comprising 764,528 nodes and 3,369,841 tetrahedral elements.

The contact surface between the distal extension removable partial denture and the gingiva was set in two different contacts. Touch contact allowed movement between surfaces with friction. In this study, only contact between the denture base and underneath soft tissue was defined as touch contact. Other contacts were defined as glued contact, which means there was no movement between surfaces. The final model was analyzed with Marc Mentat software (MSC. Software Corporation, USA).

Material properties

Co-Cr alloys have been widely used for the fabrication of the RPD skeleton due to their excellent corrosion resistance as well as suitable mechanical properties [4,5]. Homogenous isotropic linear elastic properties are assumed for parts of the prosthesis, soft tissue, and bone. The properties of the materials used in this study are shown in Table 1.

Loading conditions

The occlusal load (vertical force) of 100 N was applied vertically at the center of the occlusal surface of artificial teeth 35, 36, and 37 on the RPD (Figure 3).

Stress and strain were reported as the magnitude and distribution pattern in the form of color-contour maps. The maps demonstrated the von Mises stress distribution pattern on the cortical bone layer of the alveolar ridge and abutment tooth, and the strain distribution pattern on the cortical bone layer of the alveolar ridge.

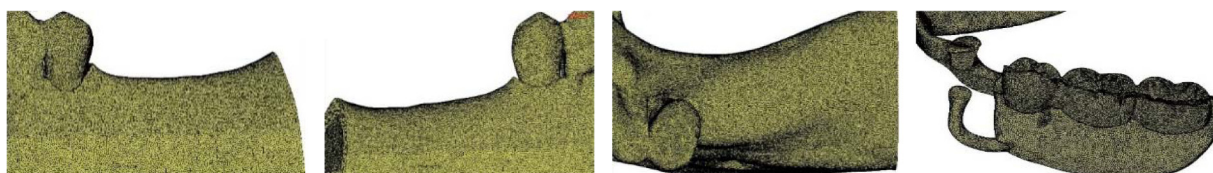


Figure 2 Section of finite element model showing nodes and elements

Table 1 Mechanical properties used for finite element analysis

Material	Elastic modulus (MPa)	Poisson's ratio
Cortical bone	13,700	0.30
Cancellous bone	1,370	0.30
Co-Cr alloys	200,000	0.33
Denture base	4,500	0.35
Soft tissue	10	0.40
Frictional coefficient between denture- soft tissue = 0.1		

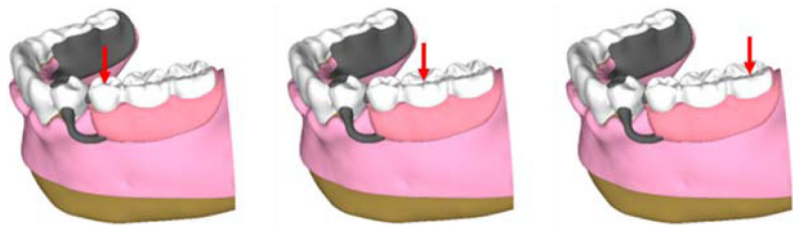


Figure 3 Location of loading force on the artificial tooth of RPD

Results


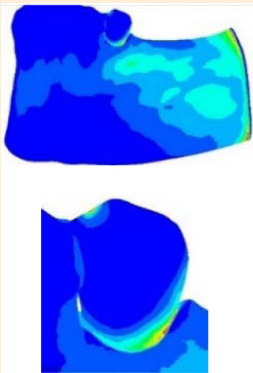
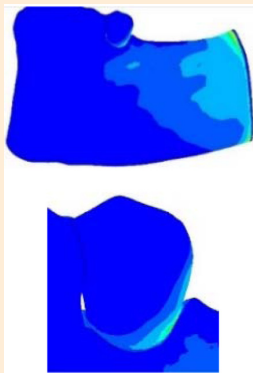
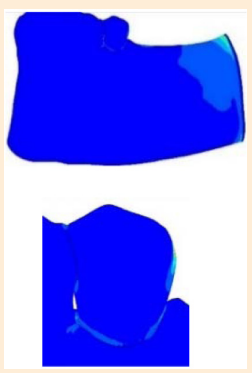
Stress distribution at the buccal aspect (Table 2)

When force was loaded on artificial tooth 35, extension of stress was observed in the area beneath the parameter of the denture base from top-to-bottom of the mandible height. The peak magnitude was located at the distal rim of the denture base. Moreover, there was stress distribution towards the anterior part of the mandible. Stress distribution was seen along the distal and cervical part of the abutment tooth. The magnitude of stress reached 4.5 MPa at the distobuccal angle at the cervical area. Stress distribution was also observed on the mesio-occlusal part of the tooth, but with less magnitude.

When force was loaded on artificial tooth 36, the same pattern of stress distribution was found onto the bearing area, but in less magnitude compared to when force was applied on artificial tooth 35. Nevertheless, there was no stress distributed to the anterior part of the mandible mesial to tooth 34. The same stress distribution pattern was observed on the abutment tooth as when force was applied on artificial tooth 35, but in less magnitude. No stress distribution was observed on the mesio-occlusal part of the tooth.

When force was loaded onto artificial tooth 37, stress was only distributed onto the alveolar bone located corresponding to the center of load and at the distal margin of the denture base. For the abutment tooth, a small magnitude of stress was observed around the distobuccal rim and the cervical part of the abutment tooth.

Table 2 Stress Distribution at the buccal view

Viewing area	Position of load		
	Artificial tooth 35	Artificial tooth 36	Artificial tooth 37
 Buccal view			



Stress distribution at the lingual aspect (Table 3)

The same pattern and magnitude of force distribution to the alveolar bone was similarly observed when force was loaded onto artificial tooth 35 or artificial tooth 36. The highest magnitude of force was observed at the bottom end of the mandible at the area corresponding to the distal rim of the denture base. When force was loaded on artificial tooth 37, the least extension and magnitude of stress was observed (compared to when the load was on other artificial teeth). Stress was only located at the upper one-fourth of the mandible height, covering the area beneath the denture base.

The highest stress on the abutment tooth was located approximately to the mesial rest and at the area of contact of the proximal plate. The more the force was applied posteriorly, the less the extension of stress was distributed to the tooth. It was shown that, when a load was on artificial tooth 37, stress was located only at the area where the proximal plate attached to the distal side of the abutment tooth.

Stress distribution at the occlusal aspect (Table 4)

When force was loaded onto artificial tooth 35 or artificial tooth 36, stress seemed to distribute with a higher magnitude toward the buccal part of the mandible and the distal end of the denture base. The least magnitude of stress distributed in the alveolar bone was observed when force was loaded onto artificial tooth 37. No matter the location of load, the highest magnitude of stress is located at the area corresponding to the middle-third part of the distal rim of the denture base.

The more the force was applied posteriorly, the less the extension of stress was distributed to the tooth. The highest stress was located at the mesial rim at the middle third of the occlusal surface, where the mesial rest was placed, and at the disto-lingual angle. Nevertheless, there was less stress at the mesial rest when force was applied at the center of artificial tooth 37.

Table 3 Stress distribution at the lingual view

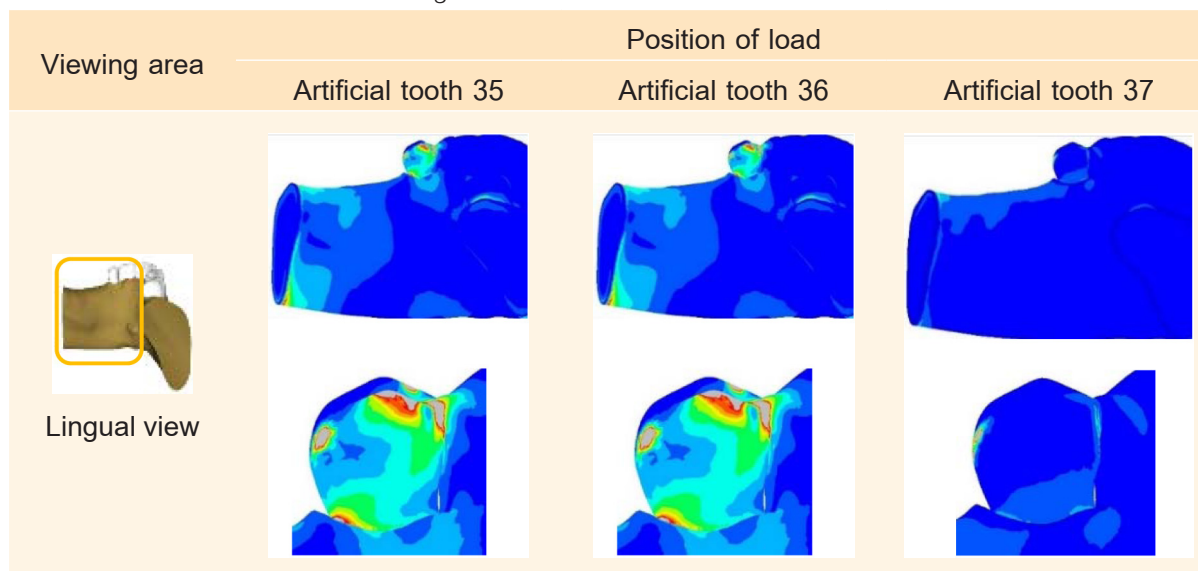
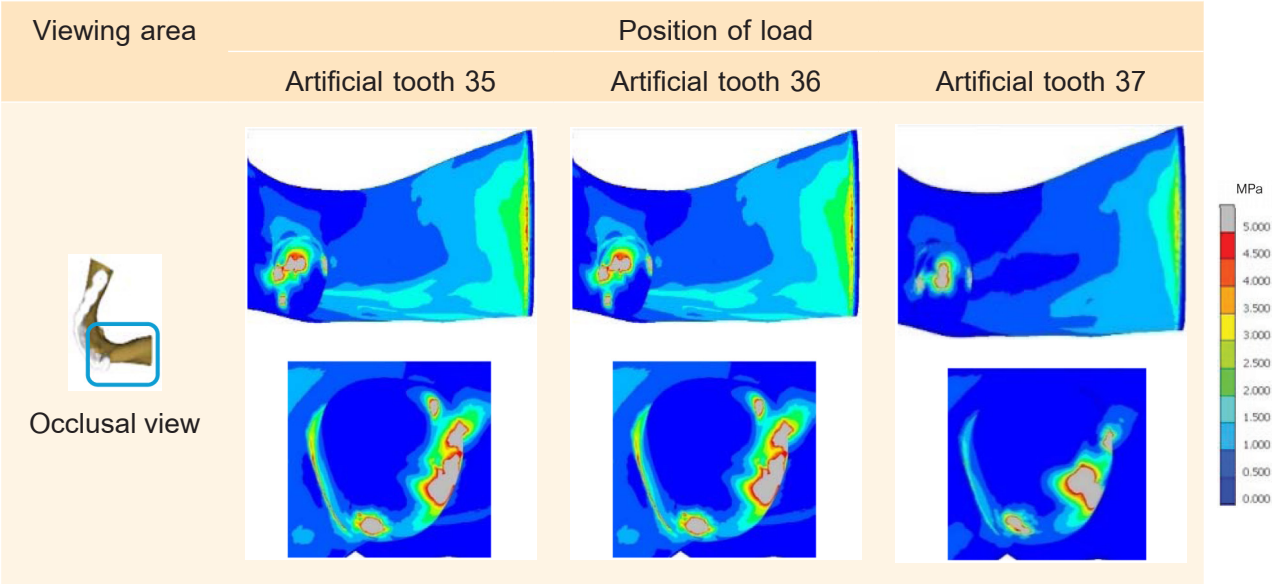


Table 4 Stress distribution at the occlusal view



Stress distribution at the posterior region (Table 5)

The highest magnitude was located towards the bottom end of the mandible, corresponding to the distal end of the denture base. A lesser magnitude of stress was observed when the center of load moved posteriorly.

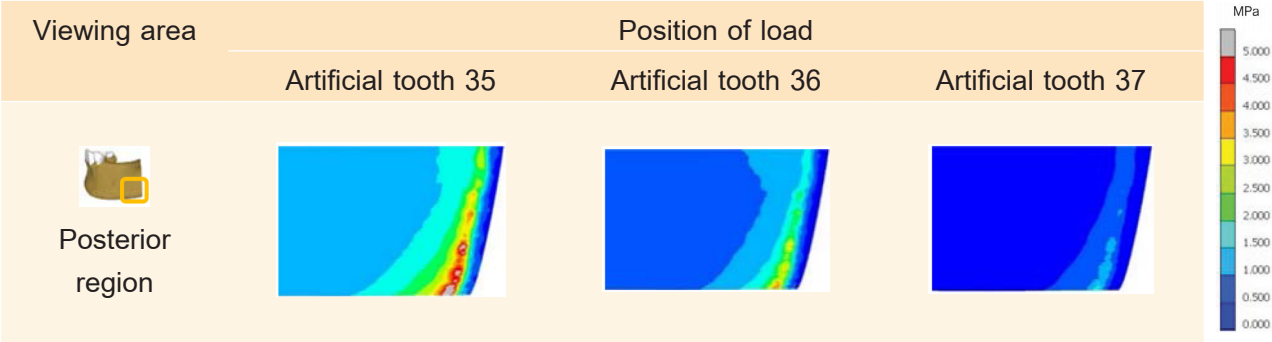
Strain distribution in the cortical bone layer

Strain distribution seemed to follow the pattern of the stress distribution but in less extension.

Discussion

This study investigated the characteristics and magnitude of stress and strain in the load-bearing area beneath the denture base of a distal extension removable partial denture (RPD). The simulation of the 3D model for the denture-bearing area (gingiva, cortical bone, spongy bone), the components of distal extension RPD (Co-Cr alloy for framework fabrication, acrylic resin for fabrication of denture base and artificial tooth), and the abutment tooth were generated.

Table 5 Stress distribution at the posterior region



Results illustrated 3D finite element analysis of stress and strain in the denture-bearing area following axial load of 100 N on a simulated artificial tooth on a Kennedy's classification II dental model. A force of 100 N was applied, as this was the average masticating force for raw cabbage, boiled meat, or cooked meat [6, 7].

Since function-induced strains could initiate cellular responses that promote perpetual bone remodeling and modeling [8, 9], our study tried to reveal the amount of stress and strain in the load-bearing area from the effect of loading force on an artificial tooth of the distal extension RPD utilizing finite element analysis (FEA). With the property of FEA, we can simulate a computer-created model to calculate stress, strain, and show the magnitude and characteristics of stress and strain distribution in the form of a color-contour map. With the versatility of FEA, the structure of all shapes can be investigated, and the stress generation can be measured at the optional points, which is difficult to do in an *in vivo* or *in vitro* study [10]. Nevertheless, the postulation of our results might not be exact since the complexity of setting up mesh models and the techniques might lead to a lack of uniform adherence of the denture base and the edentulous surface or the adhering of the mesial rest and mesial rest seat. Besides, FEA demonstrated a one-time impact force [10], which could not demonstrate the effect of continuous force during the course of denture usage.

This study explored stress distribution in the alveolar cortical bone beneath the denture base of the RPD. There was a magnitude of stress occurring in the cortical bone of the alveolar ridge supporting the denture base following the application of force on the artificial tooth of the RPD. Our results showed that the extension of stress, when applying force on artificial tooth 35, covered a larger area of the cortical bone than

when applying force on the artificial tooth located towards the posterior part of the denture base. We also explored stress distribution in the abutment tooth (tooth 34). A similar highest magnitude of stress around 5 MPa was detected in the tooth at the area where the part of the framework attached to the tooth. Stress on the abutment was also higher and spread into a larger area onto the abutment tooth when force was applied on the artificial tooth adjacent to the abutment tooth than the more distal-located artificial tooth.

According to the possible movements of the partial denture in two rotation movements (around fulcrum line axis and longitudinal axis) of the distal extension base of a tooth-tissue-supported prosthesis toward the supporting tissues when an occlusal load is applied, these functional stimulations induce alveolar bone resorption [11-13]. Ozan *et al.* [2] showed evidence of a detrimental effect of Kennedy class II prosthesis on the alveolar ridge. They found that there was both vertical and horizontal alveolar ridge resorption upon stress distribution in the RPD wearer. The dynamic of alveolar bone remodeling according to applying force was demonstrated in a review by Saffar *et al.* [14].

Following the application of occlusal load on artificial tooth, our FEA model indicated a transference of biting force to the cortical bone which demonstrated as a noticeable stress/strain concentration beneath the perimeter of the denture base along the buccal aspect through to the distal end of the denture base and in the abutment tooth. These patterns of stress and strain distribution suggested that even axial load of 100 N could move the denture base towards the supporting tissues and produce such stress and strain that potentially induce physiological tissue remodeling. From the pattern of stress and

strain distribution, the potential of cortical bone damage from biting force (strain) covered less area than the extension of force distributed into the cortical bone (stress). It could be postulated that the biting force of 100 N axially loaded on the artificial tooth closer to the abutment tooth did more damage to the cortical bone than the same magnitude of biting force on the more posterior artificial tooth. Cortical bone at the lingual aspect seemed to be the least damaged site when the biting force was on the artificial tooth adjacent to the abutment tooth. As biting force moved posteriorly, damage of the cortical bone seemed to be located mostly at the posterior region underneath the parameter of the denture base (distal end of the denture base).

The findings of our study pointed out an interesting information concerning the harmful effect of force on the artificial tooth of distal-extension RPD on tooth and surrounding periodontium. However, the difference in magnitude of stress and strain when the axial load was applied to different artificial tooth suggested that considerate and well-instructed usage of dentures could lower the detrimental effect of a Kennedy classification II prosthesis of mandibular arch to surrounding periodontium and abutment tooth, which eventually sustains the efficiency of the denture during the course of function.

Conclusion

Force applied on an artificial tooth of a distal extension RPD produced a pattern of distribution and magnitude of stress and strain that potentially exerted harmful effects on the periodontium and the abutment tooth. The avoidance of chewing hard, sticky, and difficult-to-chew food and concomitant chewing

on the far posterior artificial tooth might possibly reduce the detrimental effect on the periodontium and the abutment tooth.

Acknowledgements

We would like to extend our gratitude to Sainamthip Laboratory and Septillion 3D Lab for their support in digital technology.

Funding

The research grant for residency training program, Faculty of Dentistry, Mahidol University, Thailand

References

1. สำนักทันตสาธารณสุข กรมอนามัย กระทรวงสาธารณสุข. รายงานผลการสำรวจสภาวะสุขภาพช่องปากแห่งชาติ ครั้งที่ 8 ประเทศไทย พ.ศ. 2560. นนทบุรี:2561.
2. Ozan O, Orhan K, Aksoy S, Icen M, Bilecenoglu B, Sakul BU. The effect of removable partial dentures on alveolar bone resorption: a retrospective study with cone-beam computed tomography. *J Prosthodont.* 2013 Jan;22(1):42-48. doi: 10.1111/j.1532-849X.2012.00877.x.
3. Singhal S, Chand P, Singh BP, Singh SV, Rao J, Shankar R, *et al.* The effect of osteoporosis on residual ridge resorption and masticatory performance in denture wearers. *Gerodontology.* 2012 Jun;29(2):e1059-e1066. doi: 10.1111/j.1741-2358.2011.00610.x.
4. Chen J. Biomechanics and remodelling for design and optimisation in oral prosthesis and therapeutical procedure [thesis]. Sydney : The University of Sydney; 2014.
5. Chen X, Mao B, Zhu Z, Yu J, Lu Y, Zhang Q, *et al.* A three-dimensional finite element analysis of mechanical function for 4 removable partial denture designs with 3 framework materials: CoCr, Ti-6Al-4V alloy and PEEK. *Sci Rep.* 2019 Sep;9(1):13975. doi: 10.1038/s41598-019-50363-1.

6. Poli O, Manzon L, Niglio T, Ettorre E, Voza I. Masticatory force in relation with age in subjects with full permanent dentition: A cross-sectional study. *Healthcare (Basel)*. 2021 Jun;9(6):700. doi: 10.3390/healthcare9060700.
7. Hagberg C. Assessment of bite force: a review. *J Craniomandib Disord*. 1987; 1(3):162-169.
8. McCulloch CA, Lekic P, McKee MD. Role of physical forces in regulating the form and function of the periodontal ligament. *Periodontol 2000*. 2000 Oct; 24:56-72. doi: 10.1034/j.1600-0757.2000.2240104.x.
9. Roberts WE. Bone dynamics of osseointegration, ankylosis, and tooth movement. *J Indiana Dent Assoc*. 1999;78(3):24-32.
10. Assunção WG, Barão VA, Tabata LF, Gomes EA, Delben JA, dos Santos PH. Biomechanics studies in dentistry: bioengineering applied in oral implantology. *J Craniofac Surg*. 2009 Jul;20(4):1173-1177. doi: 10.1097/SCS.0b013e3181acdb81.
11. Alan B Carr, David T Brown. McCracken's removable partial prosthodontics. 12th ed. St.Louis, Missouri: Elsevier; 2011.
12. Mori S, Sato T, Hara T, Nakashima K, Minagi S. Effect of continuous pressure on histopathological changes in denture-supporting tissues. *J Oral Rehabil*. 1997 Jan;24(1):37-46. doi: 10.1046/j.1365-2842.1997.00443.x.
13. Reddy MS, Geurs NC, Wang IC, Liu PR, Hsu YT, Jeffcoat RL, et al. Mandibular growth following implant restoration: does Wolff's law apply to residual ridge resorption?. *Int J Periodontics Restorative Dent*. 2002 Aug;22(4):315-321.
14. Saffar JL, Lasfargues JJ, Cherruau M. Alveolar bone and the alveolar process: the socket that is never stable. *Periodontol 2000*. 1997 Feb;13:76-90. doi: 10.1111/j.1600-0757.1997.tb00096.x.